# Substrate Analogue Induced Changes of the CO-Stretching Mode in the Cytochrome P450cam–Carbon Monoxide Complex†,‡

Christiane Jung,§ Gaston Hui Bon Hoa,*,‖ Karl-Ludwig Schröder,§ Monique Simon,⊥ and Jean Pierre Doucet⊥

*Max-Delbrück-Centrum for Molecular Medicine, Robert-Rössle-Strasse 10, 1115 Berlin-Buch, FRG, INSERM-U.310, Institut de Biologie Physico-Chimique, 13 rue Pierre et Marie Curie, 75005 Paris, France, and ITODYS, UA34 CNRS, University of Paris 7, 1 rue Guy de la Brosse, 75005 Paris, France*

*Received July 10, 1992*

ABSTRACT: The CO-stretching mode of the carbon monoxide ligand in reduced cytochrome P450cam, in the absence or presence of camphor and in the presence of nine different camphor analogues, was measured at room temperature using Fourier transform infrared spectroscopy. Substrate-free cytochrome P450cam–CO reveals a broad, slightly structured band resulting from an overlap of several stretching mode signals. The multitude of the signals indicates that cytochrome P450 exists in a dynamic equilibrium of several conformational substates. Binding of camphor or camphor analogues strongly influences this equilibrium. For substrate analogues which are not able to form a hydrogen bond to the hydroxyl group of tyrosine 96, the CO-stretching band is rather broad and asymmetric. In contrast, substrate analogues with one quinone group which form a hydrogen bond to the Tyr96 OH induce a shift and a sharpening of the CO-stretching mode band. For substrate analogues with two hetero groups, the infrared spectrum is slightly asymmetric or a minor band appears. Sterical hindrance, substrate mobility, and protein flexibility finally determine the position and width of the CO-stretching mode signals.

Enzymatic catalysis is one of the most important phenomena in living organisms. Although each enzyme has its particular function and specific chemical mechanism, the question of a fundamental physical process underlying catalysis and common to all enzymes remains unanswered. Many reviews address this question (Welch, 1986; Karplus, 1986; Huber & Bennett, 1983) and attempt to relate the dynamic structural behavior of enzymes to their function. In spite of the development of physical theories and knowledge of the physical background, an experimental verification of these ideas and theories is rather complicated and often ambiguous. We suggest that the enzyme cytochrome P450 is an appropriate model for the study of the relationship between dynamics and function, both experimentally and theorically.

The term cytochrome P450 characterizes a superfamily of enzymes which catalyze the hydroxylation of different organic compounds integrated in many biosynthetic and degradative pathways in prokaryotes and eukaryotes (Ortiz de Montellano, 1986). All these enzymes consist of a thiolate iron porphyrin IX complex surrounded by a protein which differs in amino acid sequence, dependent on the species of cytochrome P450 (Nebert et al., 1991). The hydroxylation reaction catalyzed by cytochrome P450 involves several intermediate steps (Ruckpaul & Rein, 1984) (Figure 1) in which the structural requirements for cleavage of the oxygen–oxygen bond (oxygen activation) and for the insertion of the oxygen atom into the substrate carbon–hydrogen bond are not clearly understood. Most authors discuss the importance of a particular mutual sterical arrangement of the substrate and the dioxygen ligand bound to the heme iron in relation to effective catalysis (Poulos et al., 1987; Collins & Loew, 1988). Recently, however, we

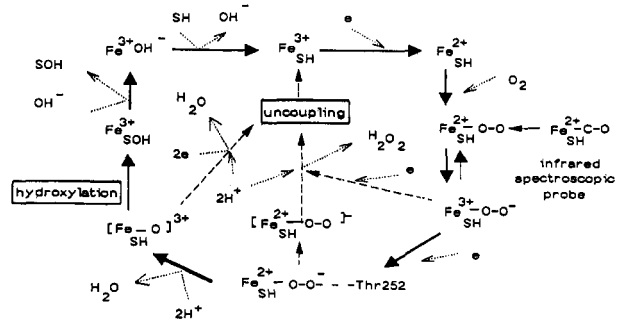


FIGURE 1: Reaction cycle of cytochrome P450cam: $Fe^{3+}$, heme group; $OH^-$, water cluster; SH, substrate.

suggested from infrared studies, using the stretching mode of the carbon monoxide ligand in ferrous cytochrome P450–CO as a spectroscopic probe, that the active site in cytochrome P450cam and P450lin exists in a dynamic equilibrium between several structural states (Jung & Marlow, 1987). We observed that both cytochrome P450 proteins dramatically differ in the temperature dependence of this dynamic equilibrium. The question remains to be the functional significance of this structural behavior. To obtain greater insight into the parameters which influence this equilibrium, we investigated the effect of pressure (Jung et al., 1991; Scholl, 1991) and substrate analogues on the CO-stretching mode bands in cytochrome P450cam. This protein is the best physicochemically characterized cytochrome P450 (Murray et al., 1985; Sligar & Murray, 1986) and the one for which the crystal structure is known (Poulos et al., 1987). It constitutes a model for the analysis of the fundamental properties of the cytochrome P450 enzyme family. Recently, the crystal structure analysis of some substrate analogue cytochrome P450cam complexes was published (Raag & Poulos, 1989a, 1991). The results indicate substantial mobility for some substrate analogues which might correlate with the loss of ability for stereospecific hydroxylation. The present paper deals with the question of whether the substrate mobility in the heme

† This work was supported by a grant from the Institut National de la Santé et de la Recherche Médicale.

‡ This paper is dedicated to Prof. I. C. Gunsalus on the occasion of his 80th birthday.

§ Max-Delbrück-Centrum for Molecular Medicine.

‖ INSERM-U. 310, Institut de Biologie Physico-Chimique.

⊥ ITODYS, UA34 CNRS, University of Paris 7.

0006-2960/92/0431-12855$03.00/0 

pocket has an influence on the equilibrium of the CO ligand conformers in reduced cytochrome P450–CO complex and whether the existence of such an equilibrium has functional consequences.

## MATERIALS AND METHODS

The gene encoding cytochrome P450cam from *Pseudomonas putida* (P450cam; new nomenclature CYP101 (Nebert et al., 1991)) was isolated (Koga et al., 1985) and expressed in *Escherichia coli* strain TB1 (Unger et al., 1986). *E. coli* cells were grown in a 30-L fermentor by a repeated batch procedure. The following conditions for running the fermentor were derived from expression studies (Unger, 1988) in flask cultures. A total of 20 L of LB-broth (10 g of tryptone, 5 g of yeast extract (Difco), 10 g of NaCl, 200 mg of ampicilin/L, pH 7.5) was completed with 800 mL of saturated aqueous camphor solution and inoculated with 1 L of inoculum, prepared from an agar slant culture and two consecutive propagations (shaking cultures, 200 mL of medium/500-mL flask). Fermentation (temperature 37 °C, pH controlled < 8.2 with 1 N HCl, $pO_2 > 5$ mg/L, antifoam poly(propylene glycol)) proceeded for 16 h. The starting cell concentration was approximately $0.5 \times 10^9$ cells/mL and increased to a final cell concentration of $9 \times 10^9$ cell/mL. At the end of the cell growth, the fermentor was cooled to 13 °C and the cell suspension was centrifuged continuously at 3 °C. A 1-L aliquot of the culture was used as inoculum for a new 20-L batch started 8 h later. The cells were washed with 50 mM phosphate buffer, pH 7, and 4% (v/v) aqueous saturated camphor solution at 3 °C and stored at −70 °C. The cell yield was 3.5 g/L (w/w). Improved yields are possible by fed batch procedures (K.-L. Schröder, unpublished results). The amount of expressed cytochrome P450 was determined directly in the cell culture from the difference absorption spectrum between the carbon monoxide and the reduced complex of cytochrome P450 using an extinction coefficient of 91 $mM^{-1}$ $cm^{-1}$ (Omura & Sato, 1964). About 6000 to 7000 nmol of cytochrome P450 are expressed in 20-L of cell culture.

The main steps in cytochrome P450 isolation and purification follow the published protocols (Gunsalus & Wagner, 1978). A total of 100 g of frozen cells was broken into small pieces and added to 200 mL of a stirred lysis mixture (final volume of 300 mL) consisting of 50 mM potassium phosphate buffer, pH 7, 200 μM *d*-camphor, 20 mM β-mercaptoethanol, 1 mM *p*-toluenesulfonyl chloride, 50 mg of lysozyme, 32 units/mL DNase I, and 3 units/mL RNase A (Sigma). The suspension was stirred at 4 °C for 10 h. Lysed cell fragments were separated by centrifugation at 10000*g* for 30 min at 4 °C. The supernatant was immediately loaded on to a DEAE anion-exchanger (Sigma) column and washed with 50 mM potassium phosphate buffer, pH 7, 5% (v/v) saturated aqueous camphor (approximately 500 μM), and 20 mM β-mercaptoethanol (twice the volume of the column), which is the standard buffer for the purification. The protein was eluated with a KCl gradient (0–250 mM). The fractions with an absorbance ratio 392 nm/280 nm of greater than 0.1 were pooled and concentrated to a final volume of about 10 mL and loaded on to a Bio-Gel P100 (fine) column equilibrated with the standard buffer. The elution fractions with a 392 nm/280 nm ratio greater than 0.6 were pooled and loaded onto a second DEAE anion-exchanger column. The protein was eluated by a KCl gradient of 0–250 mM and dialyzed against 50 mM potassium phosphate buffer, pH 7, and 500 μM camphor. The absorbance ratio 392 nm/280 nm was 1.1. Repeating the last two columns increases this value to 1.4 with, however, a loss of protein. Because the infrared measurements require high protein concentrations and are sensitive only to the active center of cytochrome P450, samples with a purification value of 1.1 were regarded as sufficiently pure for our studies.

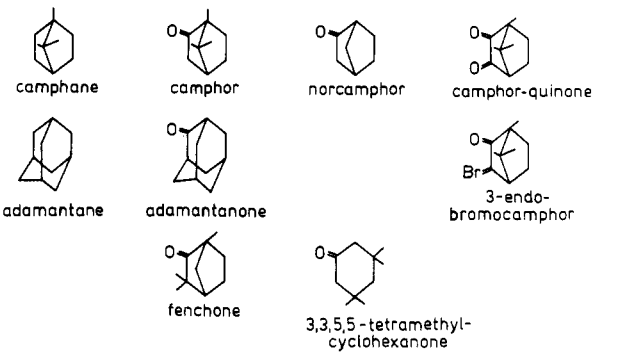


FIGURE 2: Substrate analogue structures.

Camphor was removed by dialysis of the concentrated P450 protein (approximately 1 mM) against 50 mM Tris-HCl buffer, pH 7, and 20% (v/v) glycerol, followed by Sephadex G25 (medium) chromatography run in the same buffer. Finally, the protein was dialyzed against 100 mM potassium phosphate buffer, pH 7, and 20% (v/v) glycerol and concentrated by ultrafiltration to a concentration of 1.8 mM.

Norcamphor, adamantanone, adamantanane, fenchone, camphoroquinone, 3,3,5,5-tetramethylcyclohexanone, endo-3-bromocamphor, and camphane were obtained from Aldrich-Chemie and Wiley Organics, respectively. *d*-Camphor was from Merck. Figure 2 shows the chemical structure of the substrate analogues used.

The cytochrome P450cam–carbon monoxide complex used for the infrared measurements was prepared in the following way: 50 μL of the substrate free stock solution of protein (1.8 mM) was saturated with CO by passing a strong gas stream over the surface of the solution for 6 min. A total of 2 μL of a 500 mM sodium dithionite solution (100 mM potassium phosphate buffer, pH 7, 20% (v/v) glycerol) was added. This corresponds to a 15-fold excess of dithionite to cytochrome P450. After about 2 min under the CO stream, 2 μL of an ethanolic stock solution of the substrate analogue was added into the ferrous cytochrome P450–CO complex, to yield a final substrate analogue concentration of about 20 mM. The reduced sample was then gassed with CO for a further 5 min. The sample was immediately loaded into the infrared cell consisting of two calcium fluoride windows separated by a 0.1-mm-thick Teflon spacer. The formation of the CO complex was verified directly in the infrared cell by the optical absorption spectrum. Avoiding any penetration of molecular oxygen into the infrared cell, the cytochrome P450cam–CO complex is stable for at least 4 days at room temperature without any formation of cytochrome P420. The optical spectrum before and after the infrared measurement is completely unchanged and appears for all samples like that shown in Figure 3. The determination of the cytochrome P450 concentration from the Soret band at 446 nm with the extinction coefficient of 127 $mM^{-1}$ $cm^{-1}$ (corresponding to an extinction coefficient at 417 nm in the oxidized state of 115 $mM^{-1}$ $cm^{-1}$ (Gunsalus & Wagner, 1978)) indicated an increase in the concentration of cytochrome P450 during the sample preparation from 1.8 mM to about 2.6 mM. This concentration effect was caused by the dry CO gas stream which decreased the volume of the sample solution from 50 μL down to 35 μL). This procedure of preparation of concentrated

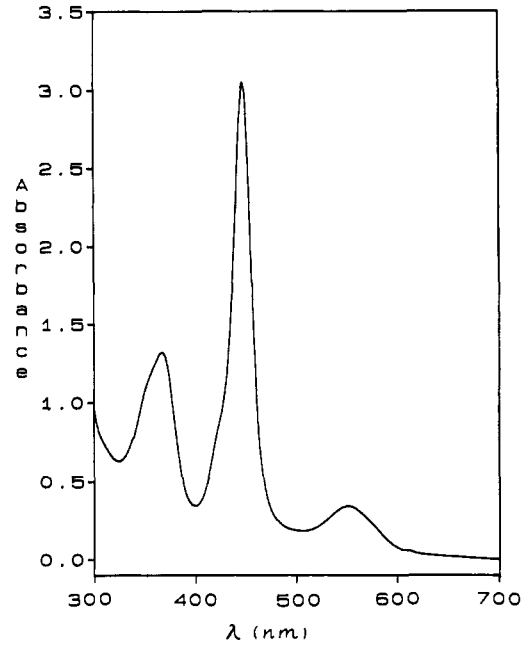


FIGURE 3: Electronic absorption spectrum of the P450cam–CO infrared samples, directly measured in the infrared cell (0.1-mm pathway, Teflon spacer, CaF windows).

P450 protein was reproducible for all infrared samples in the presence or absence of the different substrate analogues or the substrate, under the same experimental conditions. We make the assumption that only water is removed by the dry CO gas and that the extinction coefficient is independent of the concentration of the solution. We calculated the final composition of the infrared sample to be approximately 2.6 mM P450, 25 mM substrate analogue, 140 mM potassium phosphate buffer, and 12.3 mg of glycerol in 35 μL of solution (corresponding to 30% (v/v) glycerol, neglecting the contraction of the solution volume during the concentration procedure).

For the camphor-bound cytochrome P450–CO, we verified that the optical as well as the infrared spectra are similar, independent of the sequence of the substrate addition (sample preparation from a camphor-bound cytochrome P450 stock solution or addition of camphor after reduction of substrate-free cytochrome P450 as described above).

Infrared spectra were recorded on the Nicolet 60SX Fourier transform infrared spectrometer with the liquid nitrogen cooled 9010B MCT detector at 2 $cm^{-1}$ resolution. The temperature for all measurements was 19 ± 1 °C. Absorbance spectra were obtained from the ratio of the intensity spectra for the CO complexes to the intensity spectrum of the oxidized substrate-free P450 protein which does not show any bands in the spectral region between 1850 and 2050 $cm^{-1}$. The spectra were corrected by a baseline obtained by fitting the left and the right sides of the spectrum, where no CO-stretching mode bands appear (1850–1900 $cm^{-1}$ and 2000–2050 $cm^{-1}$), using a cubic polynomial function. All baseline-corrected absorbance spectra were fitted with Gaussians, Lorentzians, by a linear combination of both band shapes (Fraser & Suzuki, 1969), and by Voigtians, which represent a Lorentz–Gauss convolute (eq 1) (Voigt, 1912; Batty et al., 1976; Mantsch et al., 1986):

$$E(v_i) = \frac{1}{\pi}\int_{-\infty}^{+\infty} \exp\left(\frac{-(v-v_i)^2}{X_2^2}\right)\frac{X_1}{X_1^2+(v-v_0)^2}\,dv \quad (1)$$

with $X_1 = {}^1/_2\Delta v_{1/2}$ (Lorentz); $X_2 = {}^1/_2(\ln 2)^{-1/2}\Delta v_{1/2}$ (Gauss).

Table I: Results of the Curve Fitting (Voigt Model) of the CO-Stretching Mode Infrared Spectra

| substrate | $v$ ($cm^{-1}$) | $\Delta v_{1/2}$ ($cm^{-1}$) | shape[a] factor | population (%) | $\alpha$[b] (deg) |
|---|---|---|---|---|---|
| free | 1917.7 | 19.5 | 0.88 | 8.6 | 27 |
| | 1941.6 | 17.2 | 0.49 | 63.2 | 16 |
| | 1954.6 | 11.0 | 0.00 | 16.0 | 9 |
| | 1963.7 | 12.0 | 0.00 | 12.2 | 5 |
| adamantane | 1928.6 | 41.4 | 0.00 | 16.2 | 22 |
| | 1939.9 | 16.3 | 0.00 | 24.1 | 16 |
| | 1955.0 | 14.1 | 0.88 | 59.7 | 9 |
| camphane | 1940.9 | 10.5 | 0.86 | 11.9 | 16 |
| | 1953.7 | 14.0 | 0.00 | 88.1 | 10 |
| camphoroquinone | 1941.0 | 10.7 | 0.42 | 86.4 | 16 |
| | 1953.0 | 19.2 | 1.3 | 13.6 | 10 |
| bromocamphor | 1914.0 | 13.4 | 0.00 | 5.9 | 29 |
| | 1933.6 | 9.0 | 1.05 | 94.0 | 20 |
| camphor | 1940.6 | 12.8 | 0.32 | 100.0 | 16 |
| norcamphor | 1947.0 | 10.1 | 0.37 | 100.0 | 13 |
| fenchone | 1944.7 | 11.1 | 0.41 | 100.0 | 14 |
| adamantanone | 1942.3 | 9.1 | 0.40 | 100.0 | 15 |
| tetramethylcyclo-hexanone | 1934.2 | 9.7 | 0.40 | 100.0 | 19 |

[a] Shape factor = $(\ln 2)^{1/2}\,\Delta v_{1/2}$(Lorentz)/$\Delta v_{1/2}$(Gauss). [b] $\alpha = -0.493v + 972.847$ (angle between CO bond and heme normal) obtained as described in the Discussion.

$E(v_i)$ is the absorbance at wavenumber $v_i$. $v_0$ represents the position of the Voigtian. $\Delta v_{1/2}$ is the half-width of the Lorentzian or Gaussian. The ratio $X_1/X_2$ determines the shape factor. $X_1/X_2 = 0$ corresponds to a pure Gaussian. A pure Lorentzian is given by $X_1/X_2 \rightarrow \infty$.

For the analysis of the spectra, we attempted to find the minimum number of bands which are necessary to get a good fit. In many cases, the use of pure Gaussians or pure Lorentzians gave a poor fit. The best fit was obtained with a linear combination of Gaussians and Lorentzians or with Voigtians. Both models show the same results concerning the minimal number of bands which one has to assume for a good fit. In this paper, only the Voigtian fit data are summarized in Table I because this model describes most adequately the physical picture for the infrared absorption (Mantsch et al., 1986).

In each case, a fit was first attempted with the Gaussian lineshape which is usually observed for inhomogeneous line-broadening mechanisms (Wiersma & Duppen, 1987). It has been shown for myoglobin that the CO-stretching mode bands are inhomogeneously broadened because of the conformational substate character of the protein (Ormos et al., 1990). The quality of the fitting is demonstrated by plotting the residuals (theoretical minus experimental absorbance) in Figures 4–6. The ratio of the total area under the CO-stretching vibration spectrum to the excitation of the Soret band at 446 nm is within an error of 10%, constant for all samples, and has a value of 0.28. This indicates that the transition probability for the CO-stretching mode vibration in the different substrate-analogue-bound and substrate-free cytochrome P450 complexes is the same within the experimental accuracy. Therefore, all spectra shown in Figures 4–8 are normalized to the total area.

## RESULTS

The spectrum of the substrate-free protein is rather broad and structured, which represents an overlap of several bands (Figure 4). The distribution of the populations of the different bands depends on the solvent conditions, temperature (Jung & Marlow, 1987), and pressure (Jung et al., 1991; Scholl, 1991). The binding of the substrate and substrate analogues

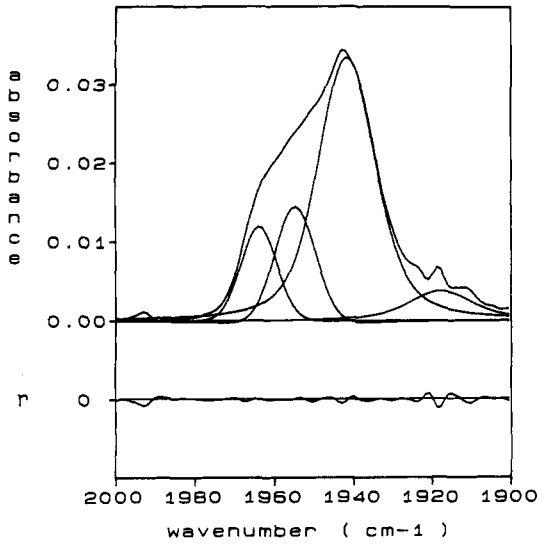


FIGURE 4: CO-stretching vibration infrared spectrum of substrate-free cytochrome P450cam–CO complex: enveloping curve, experimental spectrum; single bands, Voigtian fit; r, residuals (theoretical minus experimental spectrum).

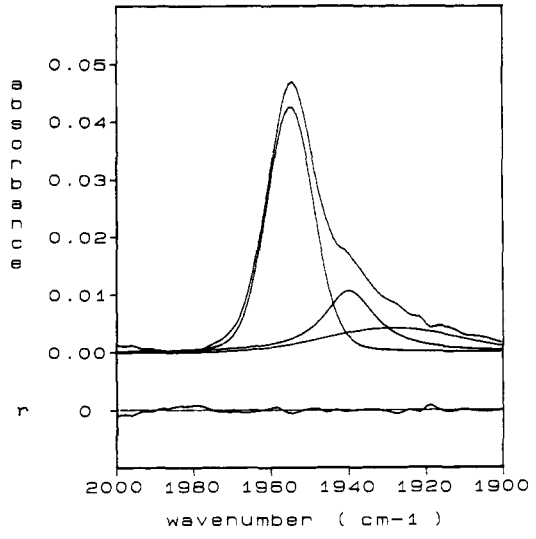


FIGURE 5: CO-stretching vibration infrared spectrum of adamantane-bound cytochrome P450cam–CO complex: enveloping curve, experimental spectrum; single bands, Voigtian fit; r, residuals (theoretical minus experimental spectrum).

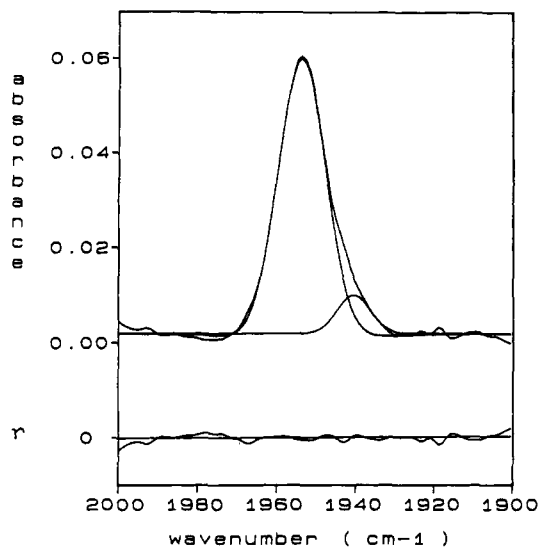


FIGURE 6: CO-stretching vibration infrared spectrum of camphane-bound cytochrome P450cam–CO complex: enveloping curve, experimental spectrum; single bands, Voigtian fit; r, residuals (theoretical minus experimental spectrum).

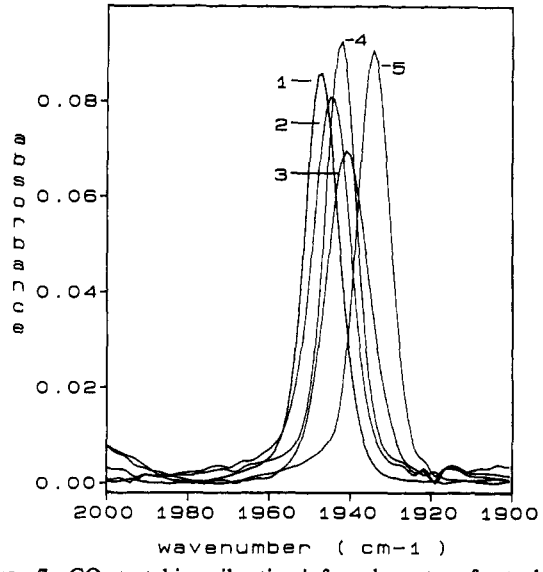


FIGURE 7: CO-stretching vibration infrared spectra of cytochrome P450cam–CO complex in the presence of the different substrate analogues: (1) norcamphor, (2) fenchone, (3) camphor, (4) adamantanone, and (5) 3,3,5,5,-tetramethylcyclohexanone.

restricts the number of the overlapping CO-stretching bands (Figures 5–8). The band position is quite different for the different substrate analogue complexes. Table I summarizes the fit results using the Voigt model. The spectrum of camphor-free cytochrome P450 has a formal half width of 33 $cm^{-1}$ and is well described by a minimal number of four bands, independent of the shape model. The bands at 1955 $cm^{-1}$ and 1964 $cm^{-1}$ are pure Gaussians (shape factor = 0). The bands at 1917 $cm^{-1}$ and 1942 $cm^{-1}$, however, show significant Lorentz shape. The lower-frequency band at 1917 $cm^{-1}$ is a real band and corresponds to the band at about 1911 $cm^{-1}$ which is resolved at low temperatures (Jung & Marlow, 1987) and is also seen in flash photolysis infrared experiments (C. Jung, unpublished results). Therefore, we exclude the possibility of a baseline artifact to be the reason for the shoulder on the lower-energy side of the spectrum. The strongly asymmetric spectrum of the adamantane-bound cytochrome P450 has a formal half-width of about 16 $cm^{-1}$ and is fitted by three Voigtians. The large half-width of 41 $cm^{-1}$ for the band at about 1929 $cm^{-1}$ may indicate an inadequate baseline correction. The other two bands, however, are real and are independent of the shape model. The camphane-bound cytochrome P450 shows a broad band with a formal half-width of about 15 $cm^{-1}$. The asymmetric shape on the lower-energy side of the band indicates an underlying band (Figure 6 and Table I).

The spectra for the protein complexes with camphor, norcamphor, fenchone, adamantanone, and tetramethylcyclohexanone (Figure 7), which show only one peak, cannot be described by a pure Gaussian or a pure Lorentzian shape. In all these spectra, a linear combination of a Gaussian and a Lorentzian as well as the Voigt model gave a good fit. The fraction of the Gaussian shape in the linear combination varies between 62% and 70% as often observed for hemoproteins (Potter et al., 1990). This is reflected in a shape factor of 0.3–0.4 for the Voigt model (Table I).

The spectra for cytochrome P450 bound with camphoroquinone or bromocamphor (Figure 8) show a relatively small

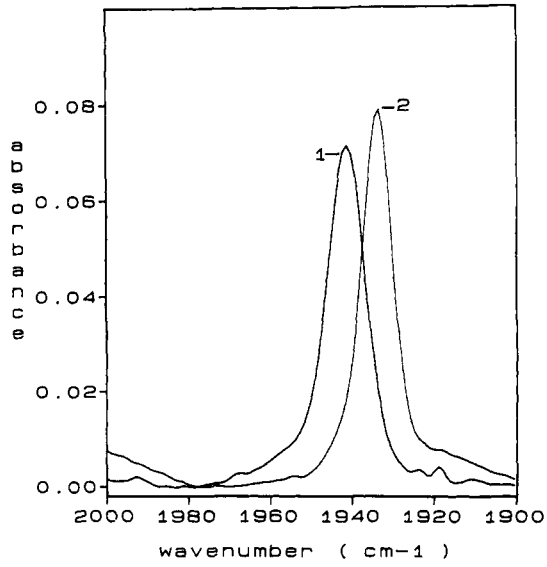


FIGURE 8: CO-stretching vibration infrared spectrum of cytochrome P450cam–CO complex in the presence of (1) camphoroquinone and (2) bromocamphor.

formal half-width between 9 and 11 $cm^{-1}$. However, the bands are asymmetric or have a shoulder, indicating a minor band.

## DISCUSSION

### *1. Substrate Mobility and CO-Stretch Vibration Multiplicity*

In this paper we reproduced earlier findings (O'Keefe et al., 1978; Jung & Marlow, 1987) that in the absence of camphor the infrared spectrum is a very broad and structured band, indicating an overlap of several signals (Figure 4). The different CO-stretching mode bands reflect different geometrical orientations of the iron-bound CO ligand which are caused by nonbonding or hydrogen-bonding contacts to the surrounding fluctuating protein (Li & Spiro, 1988) and to the small molecules occupying the heme pocket. The infrared spectra may be phenomenologically classified in four groups, according to the effect of these small molecules on the multiplicity of the CO ligand orientation.

(*i*) *Substrate-Free Cytochrome P450.* The infrared spectrum represents an overlap of at least four bands with a width between 9 and 20 $cm^{-1}$ (Figure 4). Oxidized substrate-free cytochrome P450cam posseses a water cluster at the sixth iron ligand position as has been seen in the crystal structure (Poulos et al., 1986). Until now, a crystal structure analysis of the substrate-free cytochrome P450cam–CO has not been published. However, we assume that this water cluster is not completely displaced from the heme pocket in the CO complex. These water molecules interfere with the CO ligand and induce its fluctuation within a cone around several mean orientations as sketched in Figure 9A. The mobility of the water molecules, modulated by the fluctuations of the P450 protein structure, guarantees the interconversion of the CO among these different mean orientations.

(*ii*) *Substrate Analogues Which Do Not Form a Hydrogen Bond to the Tyrosine 96 OH Group.* This group includes adamantane and camphane. The spectra are an overlap of at least two bands with a large width between 12 and 16 $cm^{-1}$ (Figures 5 and 6). We exclude the possibility that the protein is not saturated with the substrate analogues because their concentration of approximately 25 mM is 50 times greater than the dissociation constant determined for the oxidized

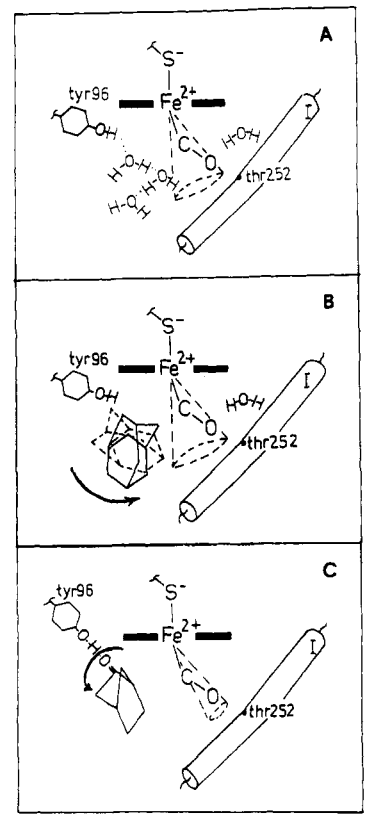


FIGURE 9: Model of the cytochrome P450cam–CO heme pocket: A, substrate-free; B, group ii, adamantane and camphane; C, group iii, norcamphor, fenchone, adamantanone, camphor, and 3,3,5,5-tetramethylcyclohexanone.

protein (46 $\mu$M for camphane (Atkins, 1988) and 50 $\mu$M for adamantane (White et al., 1984)). For the cytochrome P450 concentration of 2.6 mM, we can estimate the fraction of the substrate analogue bound protein to be 99%.

Both analogues lack the quinone group which could form a hydrogen bond to the tyrosine 96 OH group of the P450 protein as it is seen in the camphor and the adamantanone complex (Poulos et al., 1987; Raag and Poulos, 1989a). Recently, the crystal structures of the oxidized cytochrome P450cam complexed with camphane and adamantane were published (Raag & Poulos, 1991). The substrate analogues replace the water cluster except for the water molecule occupying the sixth ligand position in the oxidized state of cytochrome P450 (Raag & Poulos, 1991). This water molecule is replaced by CO in the reduced state. Adamantane and camphane are rather mobile in the heme pocket with high temperature factors of 24.7 $Å^2$ and 30.1 $Å^2$, respectively. It seems that the larger formal half-width of the bands, respective of the multiplicity of the CO ligand orientation, conforms with the substrate analogue mobility in the active center. However, the norcamphor complex, which reveals a single infrared band with a small width of 10 $cm^{-1}$, shows also a high temperature factor of 33.5 $Å^2$ (Raag & Poulos, 1989a) and therefore does not support this conclusion. Therefore, we suppose that the appearance of several overlapping infrared bands in the CO complexes indicates that camphane and adamantane themselves do not only fluctuate within one mean position but may also occupy different orientations in the CO complex (Figure 9B). Additional disordered water molecules in the heme pocket must be considered, too (Raag & Poulos, 1991). Another explanation may be derived from the recent crystal structure data of the Thr252Ala mutant and the "aged" adamantane-bound cytochrome P450 structure (Raag et al., 1991) and from molecular dynamics simulation for camphor-

bound cytochrome P450 (Paulsen & Ornstein, 1991). These studies reveal a significant flexibility of the side chains of the amino acids 248–252 in the I-helix. In this region, the I-helix shows a defect in the normal helical hydrogen bond pattern. It may be that loosely bound substrates allow a higher mobility in the I-helix groove around Thr252 by secondary effects than tightly bound substrates.

(*iii*) *Substrate Analogues Possessing Only One Quinone Group Which Forms a Hydrogen Bond to the Tyrosine 96 OH Group.* The spectrum consists of a single infrared band (Figure 7) with a width ranging between 9 and 13 $cm^{-1}$. Norcamphor, fenchone, adamantanone, camphor, and 3,3,5,5-tetramethylcyclohexanone, which show a decreasing vibration frequency in this sequence (Table I), form a hydrogen bond to the tyrosine 96 OH group as observed in the crystal structure of the respective oxidized cytochrome P450 complexes (Poulos et al., 1987; Raag & Poulos, 1989a). We assume the existence of such a hydrogen bond also for the fenchone-bound and the tetramethylcyclohexanone-bound complexes although the crystal structures for these complexes have not been published as yet. In comparison to the non-hydrogen-bonding substrate analogues, camphor and adamantanone are less mobile with temperature factors of only 16.2 $Å^2$ and 16.5 $Å^2$. This lower mobility is induced not only by the fixation of the molecules via the hydrogen bond but also by van der Waals contacts of the methyl groups in camphor with Val295 and Val247 and of the additional aliphatic ring in adamantanone with the protein. Norcamphor missing such contacts has a very high temperature factor of 33.5 $Å^2$ (Raag & Poulos, 1989a). One may conclude that norcamphor has substantial freedom for rotational fluctuations around the axis of the hydrogen bond between the norcamphor quinone group and the tyrosine 96 OH group as sketched in Figure 9C. Indeed, energy minimizations of the norcamphor–cytochrome P450 complex structure revealed two orientations of norcamphor which differ in the rotation angle around the carbon–oxygen bond of the quinone group (Collins & Loew, 1988). This kind of fluctuation of the substrate analogue may not significantly induce a multiplicity of the CO ligand orientation. In general, the picture shown in Figure 9C may be valid for all substrate analogue complexes of this group. Depending on the concrete structure of the analogues, the rotational freedom is restricted. Although we see only one infrared band, it is clear that all these bands are inhomogeneously broadened but to different extents, which reflects the substate behavior of the protein structure to exist in multiple tiers (Ansari et al., 1985). For the camphor complex, we observe the broadest band in this group with a half-width of 12.8 $cm^{-1}$. As we have shown (Jung & Marlow, 1987), cooling the sample to 20 K leads to a spectral splitting into two bands with frequencies at about 1934 $cm^{-1}$ and 1944 $cm^{-1}$. Pressure influences only the lower-frequency component (Jung et al., 1991). Furthermore, the crystal structure for camphor-bound cytochrome P450cam–CO reveals a disorder of the oxygen atom in the CO ligand (Poulos & Raag, 1989a).

(*iv*) *Substrate Analogues Possessing Several Hetero Groups.* In this group, we collect the spectra in the presence of the substrate analogues camphoroquinone and bromocamphor which cannot be clearly assigned to groups ii and iii. The spectra show a major band with an asymmetric shape which may originate from an overlap with a minor band (Figure 8). The major band may correspond to a substrate analogue orientation similar to that of camphor. The minor band in the camphoroquinone complex may result from a small fraction of molecules with a hydrogen bond between the 1-quinone group of the substrate analogue and the Tyr96 OH of the protein. In the bromocamphor complex the minor band cannot be assigned. Baseline artifacts cannot be excluded. But the band at about 1911 $cm^{-1}$ in the low-temperature studies of substrate-free cytochrome P450cam (Jung & Marlow, 1987) indicate that such a low-frequency band is possible in cytochrome P450cam. Further studies are necessary to clarify this finding.

### *2. Proximal and Distal Effects on the CO-Stretch Vibration: Conclusions for the Oxygen Activation*

It is justifiably assumed that the electronic effect of the cysteine sulfur ligand, which is in the trans position to the iron-bound CO, is the same for all substrate analogue complexes. The different CO-stretching mode frequencies must therefore result from structural changes on the distal side induced by the different substrate analogues. Similar conclusions were drawn earlier (O'Keefe et al., 1978) for camphor-bound cytochrome P450cam. Neglecting the electronic effect of the proximal ligand, a decrease in the frequency can be induced by an increase of the iron–C–O bending caused by sterical effects (Li & Spiro, 1988; Moore et al., 1988) or by an increase in the polarity of the CO ligand caused by a local electric field (Park et al., 1991; Oldfield et al., 1991). The local electric field can be induced by hydrogen bonding or by interactions with charges of distal amino acid residues of the protein.

For the camphor-bound complex, the crystal structure shows a deviation of the Fe–C bond from the heme normal, a Fe–C–O angle of about 166° with some disorder of the oxygen atom. The CO oxygen atom fits into an opening in the I-helix formed by an anomalous hydrogen bond between the threonine 252 hydroxyl group and the glycine 248 carbonyl group (Raag & Poulos, 1989b). This CO orientation corresponds to the stretching-mode frequency of about 1940 $cm^{-1}$. It was shown for myoglobin that there is a linear correlation between the wave number of the CO-stretching mode and the angle of the CO bond to the heme normal (Ormos et al., 1988). Assuming that the slope of this linear relationship is valid also for cytochrome P450cam and considering that the wavenumber of the CO stretching mode in camphor-bound cytochrome P450cam at 1940 $cm^{-1}$ corresponds to an angle of 16° (determined from the crystal structure data of camphor-bound cytochrome P450cam–CO (Poulos & Raag, 1989a)), we have calculated the average CO ligand orientation, as an angle to the heme normal, in the different substrate analogue–cytochrome P-450cam complexes to be between 5° and 29° (Table I).

The strong influence of the distal amino acids on the CO-stretch mode, which resulted in a broad shift of the CO vibration frequencies, leads again to the question of the specific role of the cysteine proximal ligand in cytochrome P450 for oxygen activation. It was concluded from quantum chemical calculations (Hanson et al., 1976; Loew & Kirchner, 1975; Jung, 1980) that the negative charge at the sulfur ligand induces a charge donation from the sulfur to the dioxygen ligand which could destabilize the O–O Bond. Using the $\pi$-INDO method (Jung et al., 1983), a net charge of the dioxygen ligand of –0.752 and –0.583 for cytochrome P450 and hemoglobin, respectively, was calculated (Jung, 1980; Rein et al., 1984). The same tendency of net charge alteration was obtained for the CO ligand (–0.223 and –0.155, respectively). The more negative net charge of CO on cytochrome P450 relative to hemoglobin leads us to predict a lower stretch vibration frequency in cytochrome P450 as compared to

Table II: Stretching Mode Frequencies for the CO and the $O_2$ Ligand in Different Hemoproteins and Model Complexes

| sample | axial ligands: fifth | axial ligands: sixth | $\nu$ ($cm^{-1}$) | reference |
|---|---|---|---|---|
| **Hemoglobin/Myoglobin** | | | | |
| human HbA | imid | CO | 1951 | Potter et al., 1990 |
| | | | 1932.0[m] | |
| | | | 1943.0[m] | |
| | | | 1969.5[m] | |
| white rabbit II Hb | imid | CO | 1951.8 | Potter et al., 1990 |
| | | | 1928.9 | |
| | | | 1970.0[m] | |
| sperm whale Mb | imid | CO | 1933.4 | Potter et al., 1990 |
| | | | 1944.0 | |
| | | | 1952.0 | Ansari et al., 1987 |
| | | | 1966.0 | |
| bovine heart Mb | imid | $O_2$ | 1103 | Maxwell et al., 1974 |
| human Hb | imid | $O_2$ | 1107 | Barlow et al., 1973 |
| **Model Complexes** | | | | |
| Fe(TpivPP) (*N*-methylimid)[a] | imid | CO | 1969 | Collman et al., 1976 |
| Fe(TpivPP) (NTrIm)[b] | imid | $O_2$ | 1163 | Collman et al., 1976 |
| heme-5 strapped heme | imid | CO | 1954 | Yu et al., 1983 |
| FeSP-15 | imid | CO | 1945 | Yu et al., 1983 |
| FeSP-14 | imid | CO | 1939 | Yu et al., 1983 |
| FeSP-13 | imid | CO | 1932 | Yu et al., 1983 |
| **Cytochrome P-450** | | | | |
| P-450cam | | | | |
| –camphor | Cys | CO | 1920.5 | this paper |
| | | | 1942.0 | this paper |
| | | | 1953.4 | Jung & Marlow, 1987 |
| | | | 1962.0 | |
| +camphor | Cys | CO | 1940.6 | |
| | Cys | $O_2$ | 1140.0 | Bangcharoenpaurpong et al., 1986 |
| P-450lin | | | | |
| –linalool | Cys | CO | 1944.3 | Jung & Marlow, 1987 |
| | | | 1955.6 | |
| | | | 1965.9 | |
| + linalool | | | 1953.0 | |
| P-450scc | Cys | CO | 1953 | Tsubaki & Ichikawa, 1985 |
| P-450lm[c] | Cys | CO | 1949 | Rein et al., 1977 |

[a] TpivPP = *meso*-tetra($\alpha,\alpha,\alpha,\alpha$-*o*-pivalamidophenyl)porphyrinato. [b] NTrIm = 1-tritylimidazole, benzene solution. [c] Solubilized phenobarbital induced rabbit P-450. Abbreviations: m, minor band; imid, imidazole; Cys, cysteine.

hemoglobin (Mincey & Traylor, 1979; Chang & Dolphin, 1976). It is seen in Table II for the CO complex of different hemoproteins that this is not observed. A similar comparison can be made for the dioxygen complex. Resonance Raman measurements on camphor-bound cytochrome P450cam (Bangcharoenpaurpong et al., 1986) revealed a single band at 1140 $cm^{-1}$; this frequency is 23 $cm^{-1}$ lower than that observed for a model complex (Collman et al., 1976) but 37 $cm^{-1}$ and 33 $cm^{-1}$ higher than that seen in hemoglobin and myoglobin, respectively (Maxwell et al., 1974; Barlow et al., 1973). Obviously, the effect of the negatively charged sulfur ligand on the electronic structure of the dioxygen complex of cytochrome P450 is still unclear.

The question arises whether an effect from the distal side, for example hydrogen bonding or polar interaction, can differentially influence the electronic structure in the prosthetic group with imidazole or mercaptide as the proximal ligand. Quantum chemical studies (Jung, 1980; Rein et al., 1984) for the distribution of an extra electron in the dioxygen heme complex (second reduction step in the reaction cycle of cytochrome P450 (Figure 1)) have shown that after reduction without previous attachment of a proton (positive charge) to the distant oxygen atom the distribution of the extra electron is similar in cytochrome P450 and hemoglobin (74–79% in the porphyrin $\pi$-system). In contrast, for both proteins the distribution of the extra electron changes significantly if a proton is bound at the distant oxygen atom of the dioxygen ligand (67% in the axial $\pi$-system for cytochrome P450, however, 68% in the porphyrin for hemoglobin). One may speculate that this electron delocalization in the axial system provides good conditions for splitting the O–O bond. Obviously, the cleavage of the O–O bond is induced by a concerted action of proximal and distal effects. A specific role of proton attachment or hydrogen bonding to the distant oxygen atom is also concluded from investigations of the camphor hydroxylation with cytochrome P450cam mutants (Imai et al., 1989; Martinis et al., 1989). Furthermore, it has been suggested from the crystal structure of the wild-type cytochrome P450 protein in the presence of different substrates (Raag & Poulos, 1991) and of the Thr252Ala mutant (Raag et al., 1991) that proton delivery to the dioxygen ligand has a different pathway for the hydroxylation and the uncoupling reaction ($H_2O_2$, $H_2O$ formation).

## ACKNOWLEDGMENT

We are very grateful to Prof. I. C. Gunsalus, University of Illinois, at Urbana–Champaign, for supplying the cytochrome P450cam clone. Drs. P. S. Stayton and S. A. Martinis from Prof. S. G. Sligar's laboratory at the Biochemistry Department of the University of Illinois, Urbana–Champaign, are acknowledged for providing the opportunity to learn the purification method for cytochrome P450cam. We thank Dr. Ritter and Gisela Sklenar for technical assistance in running the fermentor and the purification of cytochrome P450. Dr. O. Ristau is thanked for the development of the computer program for the curve fitting. C.J. is very grateful to INSERM for a short-term fellowship.

## REFERENCES

Ansari, A., Berendzen, J., Bowne, S. F., Frauenfelder, H., Iben, I. E., Sauke, T. B., Shyamsunder, E., & Young, R. D. (1985) *Proc. Natl. Acad. Sci. U.S.A. 82*, 5000–5004.

Ansari, A., Berendzen, J., Braunstein, D., Cowen, B. R., Frauenfelder, H., Hong, M. K., Iben, I. E. T., Johnson, J. B., Ormos, P., Sauke, T. B., Scholl, R., Schulte, A., Steinbach, P. J., Vittitow, J., & Young, R. D. (1987) *Biophys. Chem. 26*, 337–355.

Atkins, W. M. (1988) Ph.D. Thesis, University of Illinois, Urbana.

Bangcharoenpaurpong, O., Rizos, A. K., & Champion, P. M. (1986) *J. Biol. Chem. 261*, 8089–8092.

Barlow, C. H., Maxwell, J. C., Wallace, W. J., & Caughey, W. S. (1973) *Biochem. Biophys. Res. Commun. 55*, 91–95.

Batty, C. J., Hoath, S. D., & Roberts, B. L. (1976) *Nucl. Instrum. Methods 137*, 179–181.

Chang, C. K., & Dolphin, D. (1976) *Proc. Natl. Acad. Sci. U.S.A. 73*, 3338–3342.

Collins, J. R., & Loew, G. H. (1988) *J. Biol. Chem. 263*, 3164–3170.

Collman, J. P., Brauman, J. I., Halpert, T. R., & Suslick, K. S. (1976) *Proc. Natl. Acad. Sci. U.S.A. 73*, 3333–3337.

Fraser, R. D. B., & Suzuki, E. (1969) *Anal. Chem. 41*, 37–39.

Gunsalus, I. C., & Wagner, G. C. (1978) *Methods Enzymol. 52*, 166–188.

Hanson, L. K., Eaton, W. A., Sligar, S. G., Gunsalus, I. C., Gouterman, M., & Connell, C. R. (1976) *J. Am. Chem. Soc. 98*, 2672–2674.

Huber, R., & Bennett, W. S. (1983) *Biopolymers 22*, 261–279.

Imai, M., Shimada, H., Watanabe, Y., Matsushima-Hibiya, Y., Makino, R., Koga, H., Horiuchi, T., & Ishimura, Y. (1989) *Proc. Natl. Acad. Sci. U.S.A. 86*, 7823–7827.

Jung, C. (1980) Ph.D. Thesis, Academy of Sciences of the GDR, Berlin.
Jung, C. (1985) *Chem. Phys. Lett. 113*, 589–596.
Jung, C., & Marlow, F. (1987) *Stud. Biophys. 120*, 241–251.
Jung, C., Ristau, O., & Jung, Ch. (1983) *Theor. Chim. Acta 63*, 143–159.
Jung, C., Scholl, R., Frauenfelder, H., & Hui Bon Hoa, G. (1991) in *Cytochrome P-450: Structure & Function, Biotechnological & Ecological Aspects*, Proceedings of the 7th International Conference on Cytochrome P-450, Moscow, July 27–August 2, 1991 (Archakov, A. I., & Bachmanova, G. I., Ed.) INCO–TNC, Joint Stock Company, Moscow, 1992.
Karplus, M. (1986) *Isr. J. Chem. 27*, 121–126.
Koga, H., Rauchfuss, B., & Gunsalus, I. C. (1985) *Biochem. Biophys. Res. Commun. 130*, 412–417.
Li, X. Y., & Spiro, T. G. (1988) *J. Am. Chem. Soc. 110*, 6024–6033.
Loew, G. H., & Kirchner, R. F. (1975) *J. Am. Chem. Soc. 97*, 7388–7390.
Mantsch, H. H., Casal, H. L., & Jones, R. N. (1986) in *Spectroscopy of Biological Systems, Advances in Spectroscopy* (Clark, R. J. H., & Hester, R. E., Eds.) Vol. 13, pp 1–46, John Wiley & Sons, New York.
Martinis, S. A., Atkins, W. M., Stayton, P. S., & Sligar, S. G. (1989) *J. Am. Chem. Soc. 111*, 9252–9253.
Maxwell, J. C., Volpe, J. A., Barlow, C. H., & Caughey, W. S. (1974) *Biochem. Biophys. Res. Commun. 58*, 166–171.
Mincey, T., & Traylor, T. G. (1979) *J. Am. Chem. Soc. 101*, 765–766.
Moore, J. N. M., Hansen, P. A., & Hochstrasser, R. M. (1988) *Proc. Natl. Acad. Sci. U.S.A. 85*, 5062–5066.
Murray, R. I., Fisher, M. T., Debrunner, P. G., & Sligar, S. G. (1985) in *Metalloproteins* (Harrison, P. M., Ed.) Parts 1 and 2, Verlag Chemie, Weinheim, Basel.
Nebert, D. W., Nelson, D. R., Coon, M. J., Estabrook, R. W., Feyereisen, R., Fujii-Kuriyama, Y., Gonzalez, F. J., Guengerich, F. P., Gunsalus, I. C., Johnson, J. E. F., Loper, J. C., Sato, R., Waterman, M. R., & Waxman, D. J. (1991) *DNA Cell Biol. 10*, 1–14.
O'Keefe, D. H., Ebel, R. E., Peterson, J. A., Maxwell, J. C., & Caughey, W. S. (1978) *Biochemistry 26*, 5845–5852.
Omura, T., & Sato, R. (1964) *J. Mol. Biol. 239*, 2370–2378.
Ormos, P., Braunstein, D., Frauenfelder, H., Hong, M. K., Lin, S. L., Sauke, T. B., & Young, R. D. (1988) *Proc. Natl. Acad. Sci. U.S.A. 85*, 8492–8496.
Ormos, P., Ansari, A., Braunstein, D., Cowen, B. R., Frauenfelder, H., Hong, M. K., Iben, I. E. T., Sauke, T. B., Steinbach, P. J., & Young, R. D. (1990) *Biophys. J. 57*, 191–199.
Ortiz de Montellano, P. R. (1986) in *Cytochrome P-450—Structure Mechanism and Biochemistry*, Plenum Press, New York.
Paulsen, M. D., & Ornstein, R. L. (1991) in *Proteins: Struct., Funct., Genet. 11*, 184–204.
Potter, W. T., Hazzard, J. H., Choc, M. G., Tucker, M. P., & Caughey, W. S. (1990) *Biochemistry 29*, 6283–6295.
Poulos, T. L., Finzel, B. C., & Howard, A. J. (1986) *Biochemistry 25*, 5314–5322.
Poulos, T. L., Finzel, B. C., & Howard, A. J. (1987) *J. Mol. Biol. 195*, 687–700.
Raag, R., & Poulos, T. L. (1989a) *Biochemistry 28*, 917–922.
Raag, R., & Poulos, T. L. (1989b) *Biochemistry 28*, 7586–7592.
Raag, R., & Poulos, T. L. (1991) *Biochemistry 30*, 2674–2684.
Raag, R., Martinis, S. A., Sligar, S. G., & Poulos, T. L. (1991) *Biochemistry 30*, 11420–11429.
Rein, H., Böhm, S., Jänig, G. R., & Ruckpaul, K. (1977) *Croat. Chem. Acta 49*, 333–338.
Rein, H., Jung, C., Ristau, O., & Friedrich, J. (1984) in *Cytochrome P-450* (Ruckpaul, K., & Rein, H., Eds.) pp 163–249, Akademie-Verlag, Berlin.
Ruckpaul, K., & Rein, H. (1984) in *Cytochrome P-450*, Akademie-Verlag, Berlin.
Scholl, R. (1991) Ph.D. Thesis, University of Illinois, Urbana.
Sligar, S. G., & Murray, R. I. (1986) in *Cytochrome P-450* (Ortiz de Montellano, P., Ed.) Plenum Publishing Corp., New York.
Tsubaki, M., & Ichikawa, Y. (1985) *Biochim. Biophys. Acta 827*, 268–274.
Unger, B. P. (1988) Ph.D. Thesis, University of Illinois, Urbana.
Unger, B. P., Gunsalus, I. C., & Sligar, S. G. (1986) *J. Biol. Chem. 262*, 1158–1163.
Voigt, W. (1912) *Münich Ber.* 603.
Welch, G. R. (1986) in *The Fluctuating Enzyme*, John Wiley & Sons, New York.
White, R. E., McCartny, M. B., Egeberg, K. D., & Sligar, G. S. (1984) *Arch. Biochem. Biophys. 228*, 493–502.
Wiersma, D. A., & Duppen, K. (1987) *Science 237*, 1147–1154.
Yu, N. T., Kerr, E. A., Ward, B., & Chang, C. K. (1983) *Biochemistry 22*, 4534–4540.